CoMFA and CoMSIA Studies on 1*H*-Furan-2,5-dione and 1*H*-Pyrrole-2,5-dione as PGE$_2$ Production Inhibitor

Van Chung Pham, Min Ji Choi, Tae Woo Kim, Jungahn Kim, Dong Joon Choo, Kyung-Tae Lee,[†] and Jae Yeol Lee[*]

Research Institute for Basic Sciences and Department of Chemistry, College of Sciences,
Kyung Hee University, Seoul 130-701, Korea. [*]E-mail: ljy@khu.ac.kr
[†]Department of Pharmaceutical Biochemistry and Department of Life and Nanopharmaceutical Science,
College of Pharmacy, Kyung Hee University, Seoul 130-701, Korea
Received August 2, 2011, Accepted November 7, 2011

New generations of anti-inflammatory drugs have been developed to enhance the anti-inflammatory and analgesic activities of classic nonsteroidal anti-inflammatory drugs (NSAIDs), and to reduce the adverse effects of these agents. Selective COX-2 inhibitors are viewed enthusiastically because they match traditional NSAIDs in terms of efficacy, but circumvent constitutively active COX-1 and are comparatively free of stomach-associated complications. Diaryl-heterocycles, and other central ring pharmacophore templates, have been extensively studied as selective COX-2 inhibitors.[1] All these tricyclic molecules have 1,2-diaryl substitutions on their central hetero- or carbocyclic ring systems. The recent withdrawal of the selective COX-2 inhibitors rofecoxib and valdecoxib because of their adverse cardiovascular side effects demonstrates the need to identify new scaffolds with COX-2 inhibitory activity, but without the side effects of known agents.[2] PGE$_2$ has long been considered the principal prostaglandin of acute inflammation and of chronic diseases such as rheumatoid arthritis[3] and inflammatory bowel disease.[4] Macrophages play particularly important roles in inflammation because they produce many pro-inflammatory molecules such as PGE$_2$. Therefore, the pharmacological interference of PGE$_2$ production has been postulated as a means of alleviating a number of disease states mediated by excessive and/or protracted macrophage activation. As an attempt to discover novel compound with potent anti-inflammatory activity, therefore, we recently reported that 1*H*-furan-2,5-dione and 1*H*-pyrrole-2,5-dione derivatives showed their inhibitory activities against LPS-induced PGE$_2$ production in RAW 264.7 macrophages (Fig. 1).[5] Based on our library of syntheti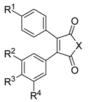c 1*H*-furan-2,5-dione and 1*H*-pyrrole-2,5-dione, in the present study, we have performed the 3-D QSAR studies on these compounds by both comparative molecular field analysis (CoMFA) and comparative molecular field similarity indices analysis (CoMSIA) method, which produce three-dimensional models to indicate the regions that affect biological activity with the change in chemical substitution.[6-8]

Among the library of 1*H*-furan-2,5-dione and 1*H*-pyrrole-2,5-dione reported by our group, 27 compounds showing a wide range of IC$_{50}$ values (0.61 to 131.53 μM) were selected for the present study. The inhibitory activities (IC$_{50}$) on LPS-induced PGE$_2$ production in RAW 264.7 macrophage cells were converted to pIC$_{50}$ (-logIC$_{50}$) values and used for both CoMFA and CoMSIA analysis. Twenty-two molecules were used as the training set and the remaining five molecules were used as the test set to validate CoMFA and CoMSIA model (Table 1). All molecular modeling calculations were performed using SYBYL-X 1.2 (winnt_os5x).[9] Energy minimizations were performed using Tripos Force Field[9,10] and Gasteiger-Huckel charge with conjugate gradient method with convergence criterion of 0.05 kcal/mol. The minimum energy conformation of entry **19** *via* simulated annealing protocol (heating molecule at 700 K for 1,000 fs and annealing molecule to 200 K for 1,000 fs) was used as a template to align the selected compounds assuming that this template is a bioactive conformation.[11] We aligned the molecules using
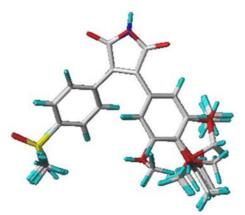

Figure 1. 1*H*-Furan-2,5-dione (X = O) and 1*H*-pyrrole-2,5-dione (X =NH).

Figure 2. Alignments based on minimum energy conformation of compound **19**.

Table 1. Structures, actual and predicted biological activities, and residuals obtained by CoMFA and CoMSIA of 1*H*-furan-2,5-dione and 1*H*-pyrrole-2,5-dione derivatives

Entry	X	R_1	R_2	R_3	R_4	IC_{50} (μM)[a]	pIC_{50}[b]	Pred. pIC_{50}		Residual[c]	
								CoMFA	CoMSIA	CoMFA	CoMSIA
Training set											
1	O	H	H	OCH$_2$O		7.13	5.1469	5.166	5.212	-0.0191	0.065
2	O	H	OMe	OMe	OMe	37.10	4.4306	4.475	4.362	-0.0444	0.069
3	O	SMe	H	H	H	3.58	5.4461	5.353	5.533	0.0931	-0.087
4	O	SMe	H	OAc	H	30.46	4.5163	4.473	4.568	0.0433	-0.052
5	O	SMe	H	OMe	H	12.60	4.8996	4.934	4.716	-0.0344	0.184
6	O	S(O)Me	H	OMe	H	23.75	4.6243	4.639	4.697	-0.0147	-0.073
7	O	SMe	H	NHAc	H	5.71	5.2434	5.295	5.201	-0.0516	0.042
8	O	SMe	H	NAc$_2$	H	78.48	4.1052	4.085	4.146	0.0202	-0.041
9	NH	H	H	H	H	27.94	4.5538	4.578	4.665	-0.0242	-0.111
10	NH	H	H	H	OMe	9.95	5.0022	5.044	4.850	-0.0418	0.152
11	NH	H	H	OMe	OMe	131.53	3.8810	3.806	4.125	0.0750	-0.244
12	NH	H	H	OCH$_2$O		7.96	5.0991	5.081	4.925	0.0181	0.174
13	NH	H	H	H	OH	13.83	4.8592	4.816	4.872	0.0432	-0.013
14	NH	H	H	OH	OH	2.69	5.5702	5.585	5.653	-0.0148	-0.083
15	NH	H	OH	OH	OH	8.19	5.0867	5.117	5.060	-0.0303	0.027
16	NH	SMe	H	H	H	4.73	5.3251	5.199	5.210	0.1261	0.115
17	NH	S(O)Me	H	H	H	21.52	4.6672	4.768	4.612	-0.1008	0.055
18	NH	S(O)$_2$Me	H	H	H	2.71	5.5670	5.685	5.734	-0.1180	-0.167
19	NH	S(O)$_2$NH$_2$	H	H	H	0.61	6.2147	6.106	6.192	0.1087	0.023
20	NH	SMe	H	OH	H	0.84	6.0757	6.058	5.975	0.0177	0.101
21	NH	SMe	H	F	H	25.50	4.5935	4.710	4.773	-0.1165	-0.180
22	NH	S(O)Me	H	F	H	45.20	4.3449	4.281	4.174	0.0639	0.171
Test set											
23	O	H	H	OMe	OMe	71.29	4.1470	4.082	4.391	0.0650	-0.244
24	O	S(O)Me	H	OAc	H	68.75	4.1627	4.181	3.935	-0.0183	0.228
25	O	S(O)$_2$Me	H	OAc	H	4.41	5.3556	4.926	5.060	0.4296	0.296
26	NH	H	OMe	OMe	OMe	25.08	4.6007	4.210	4.105	0.3907	0.496
27	NH	S(O)$_2$Me	H	F	H	10.76	4.9682	5.200	5.293	-0.2318	-0.325

[a]The inhibitory concentration on LPS-induced PGE$_2$ production in RAW 264.7 macrophage cells. [b]pIC_{50} = -log(IC_{50}). [c]Residual is defined as actual pIC_{50} - pred. pIC_{50}.

this template as shown in Figure 2.

The potential fields for CoMFA (steric and electrostatic) and CoMSIA (steric, electrostatic, donor and acceptor) were calculated at each lattice intersection of a regularly spaced grid of 2.0 Å and attenuation factor of 0.3. The regression analysis of the CoMFA and CoMSIA field energies were performed using PLS (partial least squares) with LOO (leave-one-out) cross-validation. The summary of the statistical results obtained for CoMFA and CoMSIA studies is shown in Table 2. We found that the CoMFA electrostatic descriptor played a more significant role (53.7% of contribution) than steric descriptors (46.3%) in the prediction of biological activity. A good value of 0.987 for r^2 was obtained for this model with the q^2 of 0.622. To validate the predictive power of the model derived using the training set, biological activities of the test set molecules were predicted using a test set of 5 compounds not included in the training set. The predictive ability of the model is expressed by the predictive r^2 value (0.723), which suggests that the model has good internal predictability.

The CoMSIA model with the steric, electrostatic, donor, and acceptor fields yielded unsatisfactory statistical data. The lower q^2 value of 0.362 (using six components) reveals that the model is not good. However, the conventional non-cross-validated r^2 of 0.956 and the SEE value of 0.147 indicate that this model is statistically significant. Analogous to the CoMFA, a group cross-validation was done to assess further the internal predictive ability of the model. The predictive r^2 value obtained was 0.652, which also indicated the lower robustness of this model. The cross-validated

Notes

Bull. Korean Chem. Soc. **2012**, Vol. 33, No. 1   307

Table 2. The statistical summary of PLS (Partial Least Square) analysis

Parameters	CoMFA	CoMSIA
q^2	0.622	0.362
N	8	6
r^2	0.987	0.956
SEE	0.087	0.147
F	119.626	54.487
r^2_{pred}	0.723	0.652
Fraction		
steric	0.463	0.083
electrostatic	0.537	0.389
donor		0.347
acceptor		0.181

q^2 – leave-one-out cross validated correlation coefficient; N – optimum number of components; r^2 – non cross validated correlation coefficient; SEE – standard error of estimate; F – F-test value; Fraction – relative contributions of each CoMFA/CoMSIA descriptor.
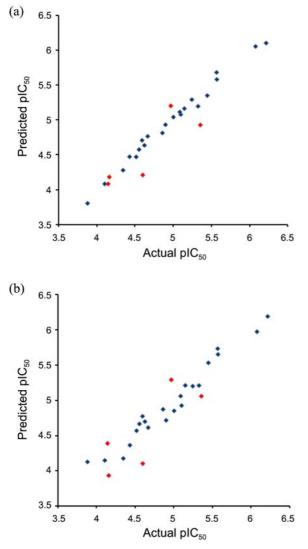

Figure 4. CoMFA steric (a) and electrostatic (b) contour plots with entry **19** (most active compound): The green contours indicate sterically favored regions whereas the yellow contours denote sterically unfavorable regions; The blue contours identify regions that favor electropositive substituents and the red regions favor electronegative substituents.

Figure 3. Correlation between cross-validated/predicted pIC_{50} versus experimental pIC_{50} for the training set (blue diamonds) and the test set (red diamonds); CoMFA (a) and CoMSIA graph (b).
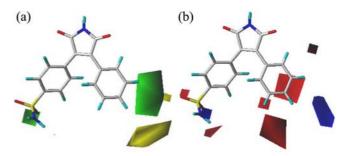
pIC_{50} values calculated by CoMFA and CoMSIA, and the residuals between the experimental and cross-validated pIC_{50} values of the compounds in the training and test set are listed in Table 1. The overall results show that the CoMFA model is better than the CoMSIA model. Plots of the cross-validated/predicted pIC_{50} versus the experimental values are shown in Figure 3. The blue diamonds and blue diamonds represent the training set and the test set, respectively.

The contour maps (Fig. 4) produced by CoMFA were analyzed by superimposing them onto compound **19** since this was the most active molecule of these series. In the CoMFA model, the fractions of steric and electrostatic fields are 46.3% and 53.7%, respectively. In Figure 4(a), green contours indicate regions where the bulky group increases activity, whereas yellow contours indicate regions where the bulky group decreases activity. The large green isopleths are located on one phenyl ring, which suggests any substituent instead of hydrogen on phenyl ring is favored (for example compound **9** *vs.* **10**). A small green polyhedron is shown in the sulfonamide moiety (for example compound **9** *vs.* **17**). Figure 4(b) shows the electrostatic contributions with compound **19** as a template ligand once again. The electrostatic contour map shows that blue contours indicate regions where the positive charge increases activity, whereas red contours indicate regions where the negative charge increases activity. A large red isopleth above the 3,4-position of phenyl ring represents an area where a negative charge is favored. This is indeed the case for compound **14** and **15** when compared to compound **9**. In particular, both red and blue areas under the sulfonamide moiety of compound **19** indicate that the sulfonamide moiety plays an important role in increasing the activity of these series compounds.

In conclusion, 3-D CoMFA and CoMSIA QSAR analyses were used to predict LPS-induced PGE_2 production inhibitory activity of a set of 1*H*-furan-2,5-dione and 1*H*-pyrrole-2,5-dione. The resultant CoMFA and CoMSIA models were validated for their predictive abilities using an external test set of five compounds. The predictive power of CoMFA model was higher than the CoMSIA model (the high predictive r^2 values of the test set). The CoMFA and CoMSIA contour maps offered enough information for us to under-

stand the various biological activities of our compound library. These 3D-QSAR models constructed in this paper can be used to guide the development of new PGE_2 production inhibitors.

References and Notes

1. Tally, J. J. *Prog. Med. Chem.* **1999**, *36*, 201.
2. Herrero, J. F.; Romero-Sandoval, E. A.; Gaitan, G.; Mazario, J. *CNS Drug Rev.* **2003**, *9*, 227.
3. Akaogi, J.; Nozaki, T.; Satoh, M.; Yamada, H. *Endocr. Metab. Immune. Disord. Drug Targets* **2006**, *6*, 383.
4. Blázovics, A.; Hagymási, K.; Prónai, L. *Orv. Hetil.* **2004**, *145*, 2523.
5. Moon, J. T.; Jeon, J. Y.; Park, H. A.; Noh, Y.-S.; Lee, K.-T.; Kim, J.; Choo, D. J.; Lee, J. Y. *Bioorg. Med. Chem. Lett.* **2010**, *20*, 734.
6. Klebe, G.; Abraham, U.; Meitzner, T. *J. Med. Chem.* **1994**, *37*, 4130.
7. Klebe, G.; Abraham, U. *J. Comput.-Aided Mol. Design* **1999**, *13*, 1.
8. Bohm, M.; Sturzebecher, J.; Klebe, G. *J. Med. Chem.* **1999**, *42*, 458.
9. SYBYL-X 1.2, Tripos Inc., 1699 Hanley Road, St. Louis, MO 63144.
10. Clark, M.; Cramer, R. D., III; Van Opdenbosch, N. *J. Comput. Chem.* **1989**, *10*, 982.
11. Crammer, R. D., III; Patterson, D. E.; Bunce, J. D. *J. Am. Chem. Soc.* **1988**, *110*, 5959.